

RESEARCH PAPER



## Elevated gut microbiome abundance of *Christensenellaceae*, *Porphyromonadaceae* and *Rikenellaceae* is associated with reduced visceral adipose tissue and healthier metabolic profile in Italian elderly

Teresa Tavella<sup>a</sup>, Simone Rampelli<sup>a</sup>, Giulia Guidarelli<sup>b</sup>, Alberto Bazzocchi<sup>c</sup>, Chiara Gasperini<sup>c</sup>, Estelle Pujos-Guillot<sup>d</sup>, Blandine Comte<sup>d</sup>, Monica Barone<sup>a</sup>, Elena Biagi<sup>a</sup>, Marco Candela<sup>a</sup>, Claudio Nicoletti<sup>e,f</sup>, Fawzi Kadi<sup>g</sup>, Giuseppe Battista<sup>b</sup>, Stefano Salvioli<sup>b,h</sup>, Paul W. O'Toole<sup>i,j</sup>, Claudio Franceschi<sup>b,k</sup>, Patrizia Brigidi<sup>l</sup>, Silvia Turrone<sup>id</sup><sup>a</sup>, and Aurelia Santoro<sup>id</sup><sup>b,h</sup>

<sup>a</sup>Unit of Microbiome Science and Biotechnology, Department of Pharmacy and Biotechnology, University of Bologna, Bologna, Italy; <sup>b</sup>Department of Experimental, Diagnostic and Specialty Medicine, University of Bologna, Bologna, Italy; <sup>c</sup>Diagnostic and Interventional Radiology, IRCCS Istituto Ortopedico Rizzoli, Bologna, Italy; <sup>d</sup>Université Clermont Auvergne, INRAE, UNH, Plateforme d'Exploration Du Métabolisme, MetaboHUB Clermont, Clermont-Ferrand, France; <sup>e</sup>Gut Health Institute Strategic Programme, Quadram Institute Bioscience, Norwich, UK; <sup>f</sup>Department of Experimental and Clinical Medicine, Section of Anatomy, University of Florence, Florence, Italy; <sup>g</sup>School of Health Sciences, Örebro University, Örebro, Sweden; <sup>h</sup>Alma Mater Research Institute on Global Challenges and Climate Change (Alma Climate), University of Bologna, Bologna, Italy; <sup>i</sup>School of Microbiology, University College Cork, Cork, Ireland; <sup>j</sup>APC Microbiome Ireland, University College Cork, Cork, Ireland; <sup>k</sup>Department of Applied Mathematics, Institute of Information Technology, Mathematics and Mechanics (ITMM), Lobachevsky State University of Nizhny Novgorod-National Research University (UNN), Nizhny Novgorod, Russia; <sup>l</sup>Department of Medical and Surgical Sciences, University of Bologna, Bologna, Italy

### ABSTRACT

Aging is accompanied by physiological changes affecting body composition and functionality, including accumulation of fat mass at the expense of muscle mass, with effects upon morbidity and quality of life. The gut microbiome has recently emerged as a key environmental modifier of human health that can modulate healthy aging and possibly longevity. However, its associations with adiposity in old age are still poorly understood. Here we profiled the gut microbiota in a well-characterized cohort of 201 Italian elderly subjects from the NU-AGE study, by 16S rRNA amplicon sequencing. We then tested for association with body composition from dual-energy X-ray absorptiometry (DXA), with a focus on visceral and subcutaneous adipose tissue. Dietary patterns, serum metabolome and other health-related parameters were also assessed. This study identified distinct compositional structures of the elderly gut microbiota associated with DXA parameters, diet, metabolic profiles and cardio-metabolic risk factors.

### ARTICLE HISTORY

Received 31 July 2020  
Revised 4 January 2021  
Accepted 11 January 2021

### KEYWORDS

Microbiota; aging; visceral adipose tissue; inflammaging; diet; serum metabolome

## Introduction


The gut microbiome is a crucial component of the individual health, by means of its impact on food degradation, energy intake, and regulation of immune system functionality.<sup>1-3</sup> Recently, the human gut microbiome has also been proposed as a determinant of healthy aging, by counteracting inflammaging (*i.e.*, the low-grade chronic inflammation characterizing the advancement of age), immunosenescence, intestinal permeability, and the decline in cognitive and bone health, thus helping to preserve homeostasis.<sup>4-9</sup>

Overall, the aged-type gut microbiome is reported to be characterized by altered diversity,

with increased representation of opportunistic bacteria and potential pathobionts, and reduced relative abundance of microbes capable of producing short-chain fatty acids (SCFAs), key signaling molecules for host metabolic and immunological homeostasis.<sup>5,10</sup> Interestingly, while the aforementioned microbiome modifications have been found to persist in longevity, in those individuals who reach the extreme limit of human lifespan (*i.e.*, semi-supercentenarians, aged >105 years), some peculiarities have emerged, that is an enrichment and/or greater prevalence of health-associated taxa, *Bifidobacterium*, *Akkermansia* and *Christensenellaceae*.<sup>11</sup> Though it is not yet clear

**CONTACT** Silvia Turrone  [silvia.turrone@unibo.it](mailto:silvia.turrone@unibo.it).

<sup>5</sup>These authors contributed equally to the work.

 Supplemental data for this article can be accessed on the [publisher's website](#).

© 2021 The Author(s). Published with license by Taylor & Francis Group, LLC.

This is an Open Access article distributed under the terms of the Creative Commons Attribution-NonCommercial License (<http://creativecommons.org/licenses/by-nc/4.0/>), which permits unrestricted non-commercial use, distribution, and reproduction in any medium, provided the original work is properly cited.

how and especially when these age-related microbiome structures are established, it is worth noting that the increased representation of health-promoting microbes in extremely old people appears to be robust to geography, as a sort of universal microbiome signature of healthy aging and longevity.<sup>12</sup>

Aging involves a series of changes in body composition, which generally result in higher levels of fat mass at the expense of muscle mass, with critical implications in terms of morbidity and quality of life.<sup>13–17</sup> Previous works, exploring how aging affects body mass distribution, have shown that muscle tissue and high-metabolic rate organs such as brain, kidneys, liver and spleen, decrease in mass with increasing age, while the abdominal area is more prone to fat deposits.<sup>14,18</sup>

The elderly indeed tend to accumulate fat in the muscles, liver and viscera as lipid droplets, while losing subcutaneous fat mass.<sup>15</sup> The age-related accumulation of fat deposition has been associated with an increase in a pro-inflammatory state that may contribute to the onset of cardiovascular disease, insulin resistance and type 2 diabetes.<sup>19,20</sup> In particular, evidence has shown that excess visceral adipose tissue (VAT) rather than accumulation of subcutaneous adipose tissue (SAT), represents the cause of atherosclerotic cardiovascular events and is the key contributor to metabolic syndrome.<sup>21,22</sup>

The accumulation of fat mass is also well known to be linked to the gut microbiota. Landmark studies in animal models revealed that microbial transplantation from obese to lean mice was able to induce weight gain.<sup>23,24</sup> More recently, findings in human subjects showed that lean and obese individuals have a particular gut microbial signature in terms of composition and diversity with also differences between men and women.<sup>25–28</sup> Furthermore, in one of the largest gut microbiota-obesity studies to date, conducted in a cohort of twins, the authors suggested the existence of heritable microbes that could play a major role in components of adiposity relevant for cardiovascular risk.<sup>29</sup> However, these studies have mostly dealt with individuals with a wide age range, so the associations between microbiome and fat distribution in the elderly are still poorly understood.

Measures specifically assessing visceral fat could help better explore the contribution of the gut

microbiome to abdominal adiposity. In this regard, different imaging methods such as ultrasound, computed tomography (CT) and magnetic resonance, are able to assess VAT and SAT, being CT the “gold standard” technique for assessing this. However, CT is limited by radiation exposure and availability and MRI is limited in terms of availability. Dual-energy X-ray absorptiometry (DXA) is considered the “gold standard” technique for body composition assessment at molecular level – translated into a 3-compartment model of fat mass, non-bone lean mass and bone mineral content, and certain DXA devices have embedded algorithms to specifically estimate the amount of VAT and SAT in the android region.<sup>17,30</sup> Unlike indirect measures, such as the body mass index (BMI), DXA allows rapid, sensitive and accurate, yet non-invasive, characterization of body composition, including levels of fat and lean mass, and bone density.<sup>31</sup>

In an attempt to better reveal the associations between abdominal adiposity and gut microbiome in old age, here we analyzed the multivariate relationship between DXA-derived measures of VAT and SAT and the gut microbiota structure, as profiled by 16S rRNA gene-based sequencing, in a cohort of 201 Italian seniors, enrolled within the EU FP7 NU-AGE project. Dietary data, collected by 7-day food records, and serum metabolomics data, generated by ultra-performance liquid chromatography coupled to quadrupole-time-of-flight mass spectrometer, were also analyzed to explore associations of macro/micronutrients and metabolites with abdominal adiposity-related microbiota profiles. We find that distinct gut bacterial taxa are associated with reduced VAT, as well as with peculiar profiles of circulating metabolites and food intake. Monitoring and possibly modulating the gut microbiota, in addition to promoting healthy eating habits, could therefore represent an additional tool to support healthy aging and possibly longevity.

## Results

To explore microbiome links to abdominal adiposity in the elderly, we profiled the fecal microbiome and searched for its correlations with DXA-derived parameters describing fat, in

particular visceral and subcutaneous adiposity, and lean mass composition, in a cohort of 201 elderly subjects (101 females, 100 males; age range, 65–79 years, mean age, 71.2 years) from the Emilia-Romagna region (Italy), in the context

of the NU-AGE FP7 EU project (see Table 1 for cohort description). Our microbiota dataset was composed of 15,167,630 high-quality reads with an average of 75,460 ( $\pm$  64,658, SD) 300-bp paired-end reads per sample.

**Table 1.** Demographic, anthropometric, biochemical and other health-related parameters in a cohort of 201 Italian elders. Data are shown for the entire cohort as well as for the three microbiome groups (G1 to G3), as identified by PCoA of unweighted UniFrac distances (see Figure 1a). Values are expressed as mean (SD), unless otherwise indicated. *P* values were determined by Kruskal-Wallis test, followed by post-hoc Wilcoxon test. HOMA-IR, homeostasis model assessment of insulin resistance. ns, not significant.

	All (no. = 201)	G1 (no. = 147)	G2 (no. = 20)	G3 (no. = 34)	<i>p</i> value
Age (years)	71.2 (3.8)	71.2 (3.7)	70.9 (3.8)	71.4 (4)	ns
Gender (M/F)	101/100	67/80	14/6	20/14	ns
<b>Anthropometry</b>					
Frailty status (Pre-frail/Non-frail)	46/155	32/115	4/16	10/24	ns
Weight (kg) <sup>#§</sup>	72.9 (13)	73.5 (13)	64.3 (11.3)	75.8 (13)	0.007
Height (m)	1.64 (0.1)	1.65 (0.1)	1.61 (0.1)	1.63 (0.1)	ns
Body Mass Index (BMI, kg/m <sup>2</sup> ) <sup>#§</sup>	27.04 (3.7)	27.04 (3.60)	24.68 (3.25)	28.48 (4.18)	0.002
Waist circumference (cm) <sup>#§</sup>	92.74 (11.63)	93.12 (11.63)	84.75 (9.31)	95.79 (11.05)	0.003
Hip circumference (cm) <sup>§^</sup>	101.63 (7.78)	101.43 (7.75)	97.58 (7.36)	104.75 (7.04)	0.004
Waist/hip ratio <sup>#</sup>	0.91 (0.09)	0.92 (0.09)	0.86 (0.07)	0.91 (0.08)	0.023
<b>Physical function</b>					
Hand grip strength (kg)	31.13 (9.69)	31.71 (9.19)	28.59 (7.88)	30.14 (12.37)	ns
Activities of Daily Living (ADLs) score	5.83 (0.38)	5.84 (0.37)	5.90 (0.31)	5.74 (0.45)	ns
Instrumental Activities of Daily Living (IADLs) score	6.51 (1.50)	6.37 (1.50)	7.10 (1.41)	6.76 (1.50)	ns
Physical Activity Scale for the Elderly (PASE) score	117.71 (71)	118.22 (51.57)	125.03 (45.69)	110.99 (48.49)	ns
<b>Inflammation</b>					
c-Reactive Protein (CRP, log odds)	0.20 (0.97)	0.23 (0.99)	0.08 (1.05)	0.12 (0.83)	ns
Pentraxin-3 (log odds)	0.11 (1.03)	0.09 (1.07)	0.45 (0.69)	0.07 (1.00)	ns
Adiponectin (log odds) <sup>#§</sup>	0.19 (0.91)	0.12 (0.87)	0.89 (0.66)	0.09 (1.03)	0.001
Leptin (log odds)	−0.03 (0.92)	−0.07 (0.92)	−0.22 (0.91)	0.24 (0.89)	ns
Ghrelin (log odds)	−0.29 (0.94)	−0.35 (0.96)	0.01 (0.78)	−0.19 (0.94)	ns
<b>Glucose metabolism</b>					
Insulin (mU/mL)	9.65 (6.88)	9.91 (7.28)	7.45 (4.96)	9.79 (5.92)	ns
Glucose (mmol/L)	5.77 (0.79)	5.80 (0.77)	5.61 (0.98)	5.74 (0.75)	ns
HOMA-IR	2.54 (1.98)	2.64 (2.13)	1.83 (1.19)	2.53 (1.60)	ns
<b>Lipid metabolism</b>					
Total cholesterol (g/L)	1.98 (0.33)	1.96 (0.33)	2.02 (0.37)	2.02 (0.34)	ns
High-Density Lipoprotein (HDL, g/L)	0.56 (0.15)	0.56 (0.16)	0.63 (0.15)	0.54 (0.14)	ns
Low-Density Lipoprotein (LDL, g/L)	1.21 (0.28)	1.19 (0.28)	1.22 (0.29)	1.27 (0.28)	ns
Triglycerides (g/L)	1.04 (0.41)	1.06 (0.42)	0.88 (0.36)	1.04 (0.35)	ns
Total cholesterol/HDL ratio	3.72 (1.04)	3.74 (1.07)	3.31 (0.79)	3.88 (0.98)	ns
<b>Cardiovascular function</b>					
Systolic pressure (mmHg)	133.25 (16.36)	133.65 (16.43)	129.68 (15.98)	133.64 (16.51)	ns
Diastolic pressure (mmHg) <sup>#</sup>	73.43 (9.23)	74.43 (9.43)	69.32 (7.71)	71.51 (8.35)	0.014
Heart rate (bpm)	68.77 (9.59)	68.70 (9.86)	69.78 (8.24)	68.48 (10.14)	ns
Homocysteine (μmol/L)	15.06 (8.51)	14.37 (3.57)	14.36 (3.55)	18.44 (19.01)	ns
<b>Renal function</b>					
Albumin (g/L)	43.84 (2.61)	44.05 (2.49)	42.73 (3.05)	43.60 (2.71)	ns
Creatinine (μmol/L) <sup>#</sup>	77.35 (18.21)	79.09 (17.89)	69.45 (16.98)	74.56 (19.21)	0.022
Uric acid (mg/24 h) <sup>#§</sup>	312.07 (69.99)	320.09 (66.57)	254.83 (56.77)	311.51 (76.98)	0.000
<b>Liver function</b>					
Alkaline phosphatase (ALP, μkat/L)	1.24 (0.29)	1.23 (0.30)	1.21 (0.25)	1.30 (0.25)	ns
Gamma-glutamyl transpeptidase (GGT, μkat/L)	0.43 (0.24)	0.42 (0.23)	0.44 (0.35)	0.43 (0.21)	ns
Aspartate aminotransferase (AST, μkat/L)	0.43 (0.10)	0.44 (0.11)	0.44 (0.09)	0.42 (0.08)	ns
Alanine transaminase (ALT, μkat/L)	0.57 (0.15)	0.58 (0.16)	0.57 (0.13)	0.55 (0.11)	ns
<b>Cognitive function</b>					
Cambridge Mental Disorders of the Elderly Examination (CAMDEX), subjective memory score	3.83 (1.96)	3.86 (1.99)	3.85 (2.35)	3.68 (1.61)	ns
Geriatric Depression Scale (GDS) score	2.34 (2.37)	2.19 (2.13)	2.30 (2.54)	3.00 (3.10)	ns
Mini Mental State Examination (MMSE) score	28.44 (1.38)	28.38 (1.39)	28.90 (1.12)	28.41 (1.48)	ns

Post-hoc Wilcoxon test: <sup>#</sup>G1 vs G2, *p* value < 0.05; <sup>§</sup>G2 vs G3, *p* value < 0.05; <sup>^</sup>G1 vs G3, *p* value < 0.05.

Overall, the gut microbial profiles showed a high representation of the phylum Firmicutes (mean relative abundance, 80%), along with Bacteroidetes (8.9%) and Actinobacteria (7.4%). The *Ruminococcaceae* (37.5%) and *Lachnospiraceae* (27.6%) families, both belonging to Firmicutes, were the most represented in the dataset. At the genus level, *Subdoligranulum* (12.5%), *Faecalibacterium* (7.8%) and *Bifidobacterium* (4.6%) were identified as the most abundant taxa (please see Fig. S1 for phylum-, family-, and genus-level profiles).

When examining the beta diversity of microbial communities by PCoA of unweighted UniFrac distances, we identified three distinct groups of individuals, *i.e.*, G1 to G3 (Figure 1a). Within a range of microbiota profiles, these groups represent clusters of subjects who have a significantly different microbiota structure from each other, as demonstrated by the permutation multivariate analysis of variance

(permutational test with pseudo-F ratio,  $R^2 = 0.25$ ,  $p$  value = 0.0001). The separation of the three groups was further verified by hierarchical clustering with Ward as the linkage method (Fisher's exact test,  $p$  value < 0.0001) (Fig. S2). The stability of the clusters was supported by average Jaccard similarities from 1000 bootstrappings of 0.96 (G1), 0.95 (G2) and 0.92 (G3). The groupings were also evaluated by weighted and generalized UniFrac metrics, by verifying rejection of the null hypothesis (*i.e.*, no difference between the three predefined clusters) ( $p$  value = 0.0001) (Fig. S3).

The three groups were also found to differ in alpha diversity, with G2 and G3 samples showing the highest values, according to the number of observed Amplicon Sequence Variants (ASVs) and the Chao1 index (Kruskal-Wallis test,  $p$  value = 0.05; post-hoc Wilcoxon test,  $p$  value = 0.045 for both G1 vs G2, and G1 vs G3) (Fig. S4). Such values were associated with

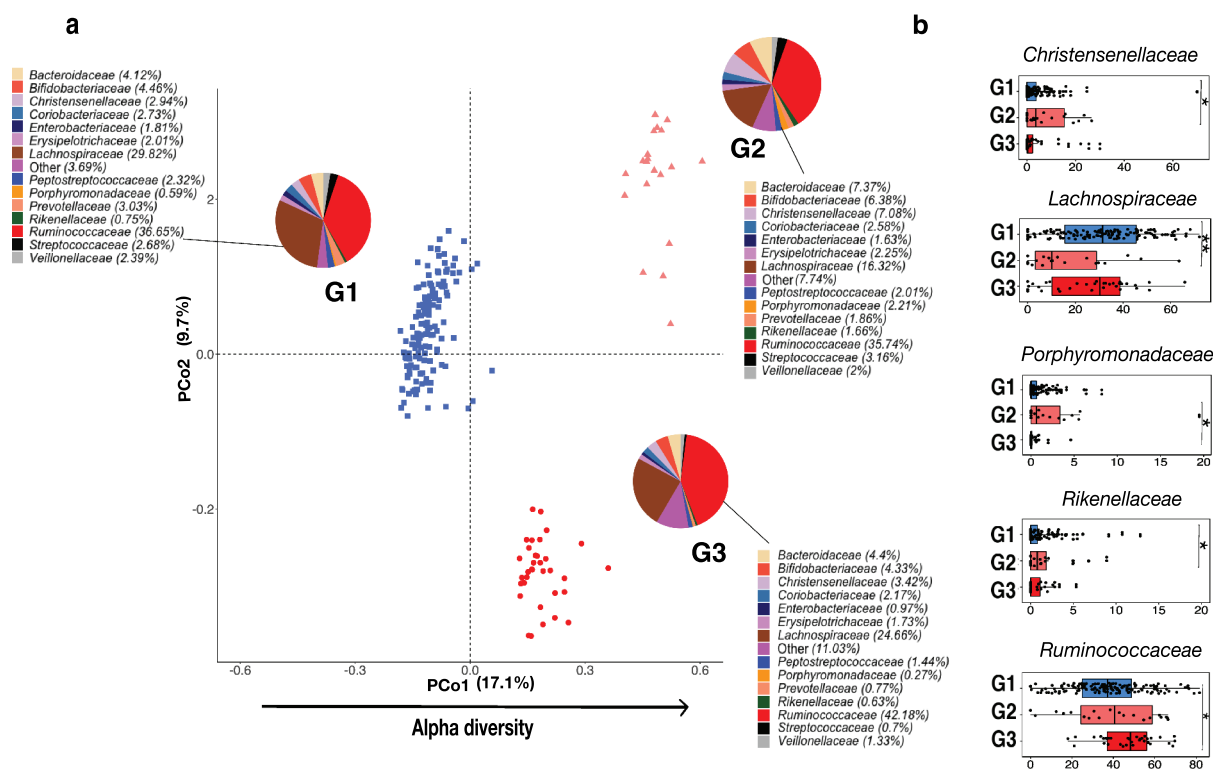


**Figure 1.** Gut microbiome profiles in Italian elders. a. Principal Coordinates Analysis (PCoA) plot based on the unweighted UniFrac distances of the fecal microbiota profiles of 201 elderly Italians. Three groups with a significantly different microbial community structure were identified (permutational test with pseudo-F ratio,  $p$  value = 0.0001). We refer to them as G1, G2, G3 based on their self-organization in the PCoA space (*i.e.*, left, right upper and lower right quadrant, respectively). The pie charts in the plot summarize the family-level relative abundances in the three groups, considering only the taxa present in at least 20% of the samples (*i.e.*, 40 individuals) with  $\geq 0.1\%$  relative abundance. The arrow at the bottom of the PCoA plot represents the alpha diversity gradient, estimated as number of observed ASVs. b. Box-and-whisker plots of relative abundances of families differentially represented among the three microbiome groups. \* respectively  $p$  value < 0.01 and < 0.05, Wilcoxon test.



the microbiome space, meaning that the sample coordinates on the PCoA plot of [Figure 1a](#) also mirrored the differences in diversity among the three groups (linear regression analysis,  $p$  value = 0.02 for the number of observed ASVs, and  $p$  value = 0.01 for Chao1 index). In particular, we observed a gradual increase in diversity along PCo1, from the lowest values in G1 microbiomes to the highest values in the samples belonging to the G2-G3 clusters.

As mentioned above for the entire cohort, the fecal microbiota of all groups was largely dominated by only two families, *Ruminococcaceae* and *Lachnospiraceae*, even if with different proportions ([Figure 1b](#)). The relative abundance of *Ruminococcaceae* was in fact significantly greater in G3 compared to G1, while that of *Lachnospiraceae* was lower in G2 compared to G1 (Wilcoxon test,  $p$  value  $\leq$  0.01). The three groups were also found to differ in subdominant families. In particular, G2 showed an enrichment in *Christensenellaceae* and *Rikenellaceae* compared to G1, as well as in *Porphyromonadaceae* compared to G3 ( $p$  value  $\leq$  0.05).

It is important to note that the stratification in the three groups was independent of gender and frailty (pairwise Fisher's exact test,  $p$  value  $>$  0.05) as well as age (Kruskal-Wallis test,  $p$  value  $>$  0.05) (see [Table 1](#) and [Fig. S5](#)). Moreover, as shown in [Table 1](#), the three groups were similar for the majority of the measured parameters related to physical function, glucose and lipid metabolism, liver and cognitive function ( $p$  value  $>$  0.05). However, the elderly subjects in G2 group compared to G1 and G3 showed significantly lower values for anthropometric measures (*i.e.*, BMI, waist and hip circumference and waist-to-hip ratio), cardiovascular risk factors (diastolic pressure), renal function markers (creatinine and uric acid) and higher values for adiponectin (an adiposity-related cytokine with anti-inflammatory effects) (post-hoc Wilcoxon test,  $p$  value  $<$  0.05) ([Table 1](#)). The number of subjects taking medicines was similar for antihypertensive drugs (G1: 77.5%, G2: 80.0% and G3: 73.5%) in the three groups, while a higher number of elderly in the G3 group had taken statins (G1: 17.0%, G2: 15.0% and G3: 26.5%), and no elderly in the G2 group had taken anti-diabetic drugs (G1: 8.8%, G2: 0% and G3: 5.9%).

We then explored the associations between the three microbiome profiles and the DXA-derived body composition variables, with a specific focus on abdominal fat. The elderly in G2 group showed significantly lower levels of VAT than G1 and G3 subjects ( $p$  value = 0.003) while no differences were observed with respect to SAT ( $p$  value = 0.2) ([Figure 2a](#)). Accordingly, the VAT/SAT ratio was significantly lower in G2 compared to G1 and G3 subjects ( $p$  value  $<$  0.05) ([Figure 2a](#)). Consistent results were also observed for the other DXA variables related to adiposity ([Fig. S6](#)). Correlations between DXA metadata and relative abundances of genus-level taxa were then specifically sought by means of sPLS regression ([Figure 2b and 2c](#)). Genera belonging to *Christensenellaceae* (*Christensenellaceae* R7 group), *Porphyromonadaceae* (*Parabacteroides*) and *Rikenellaceae* (*Alistipes*), *i.e.*, the families found to be enriched in the fecal microbiota of G2 subjects, were inversely associated with a number of DXA variables, including VAT. On the other hand, members of the *Lachnospiraceae* family (*Eubacterium rectale* group, *Fusicatenibacter* and *Blautia*), whose proportions were far lower in the G2 group, were positively correlated with the vast majority of the considered DXA measures, including especially those related to fat mass distribution (*i.e.*, whole-body fat mass (FM), whole-body fat mass index (FMI), android fat mass to android lean mass ratio (AF/AL), android fat mass to gynoid fat mass ratio (AF/GF) and VAT). Discordant data were instead observed for *Ruminococcaceae*, an overrepresented family in the G3 group, with three genera (*Ruminococcaceae* UCG 014, 002, 005) negatively and three others (*Faecalibacterium*, *Subdoligranulum* and *Ruminococcus* 2) positively correlated with most of the adiposity-related DXA variables. Finally, it should be noted that the lean mass parameter SMI (skeletal mass index, *i.e.*, the appendicular lean mass to total body mass ratio) differed from all the others, both for the position in the correlation circle plot and for the direction of correlations. In particular, a direct correlation was observed for *Christensenellaceae* R7 group, as well as for three *Ruminococcaceae* genera (*Ruminococcaceae* UCG 014, 002, 005). On the other hand, consistent with the observations above, *Ruminococcus* 2, *Subdoligranulum* and the *Lachnospiraceae* members

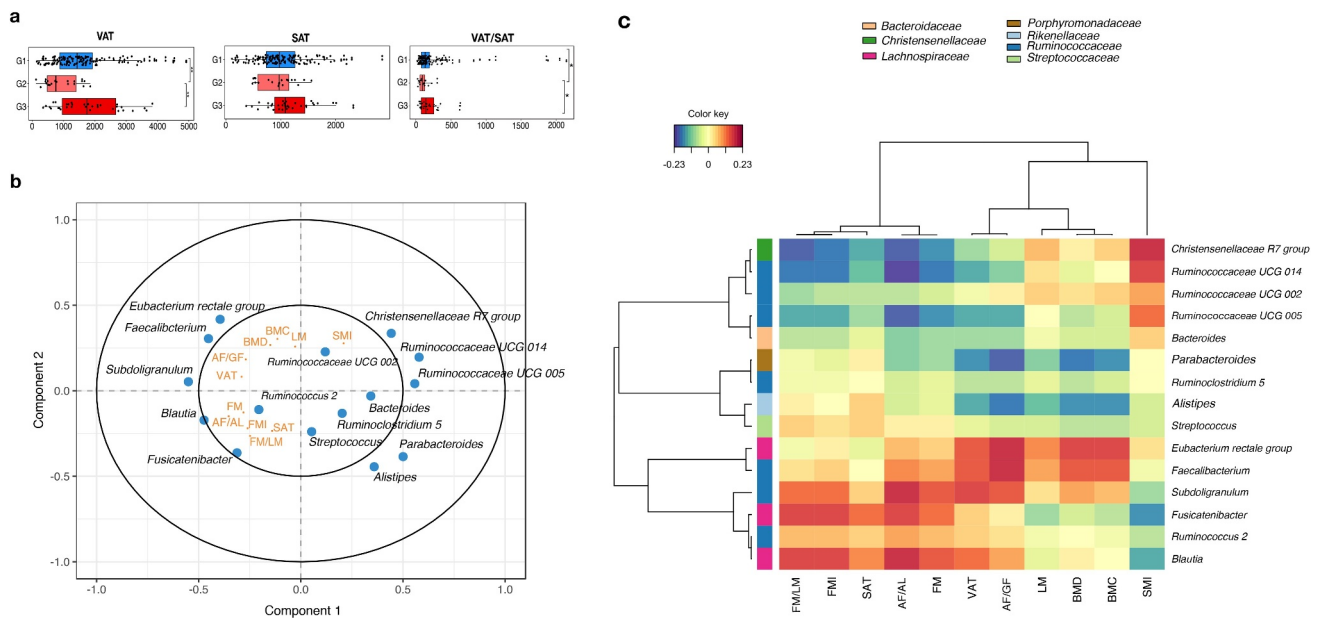


**Figure 2.** Associations between the elderly gut microbiome and body composition. **a.** Box-and-whisker plots of visceral adipose tissue (VAT, g) and subcutaneous adipose tissue (SAT, g) measures, and their ratio, for the three microbiome groups identified by unweighted UniFrac-based PCoA of Figure 1a (i.e., G1 to G3). \*\*\* respectively  $p$  value < 0.01 and 0.05, Wilcoxon test. **b.** Sparse partial least square (sPLS) regression of microbial abundances at the genus level and DXA variables. Correlation circle plot for the first two sPLS components with correlations depicted for  $< -0.2$  and  $> 0.2$ . The two circumferences show correlation coefficient radii at 0.5 and 1.0. The farther from the center a bacterial genus or DXA measure is, the greater the association with the component. Variables projected in the same direction of the plot are positively correlated, while variables in diametrically opposite position are negatively correlated. Variables located perpendicular to each other are not correlated. The variance explained by the genera is 10% on the first component and 5% on the second component, while the variance explained by the DXA variables is 37% on the first component and 42% on the second component. **c.** Hierarchical clustering obtained with complete linkage method and Pearson correlation as distance, was performed on the sPLS regression model retaining the variables shown in the correlation circle plot. For each genus, family level assignment is also shown (see color legend). The abbreviated names of the DXA variables correspond to whole body fat mass (FM), whole body fat mass index (FMI), whole body fat mass to lean mass ratio (FM/LM), whole body lean mass (LM), appendicular lean mass to total body mass ratio (SMI), whole body bone mineral content (BMC), whole body bone mineral density (BMD), android to gynoid fat mass ratio (AF/GF), android fat mass to lean mass ratio (AF/AL), visceral adipose tissue (VAT), and subcutaneous adipose tissue (SAT).

*Fusicatenibacter* and *Blautia* negatively correlated with SMI.

Seven-day food records were used to assess dietary intake. The results were normalized to the body weight of the individuals, facilitating a comparison among the three microbiome groups. The dietary intakes of nutrients for G1, G2 and G3 are shown in Table 2. No significant differences were found for the total intake of energy, saturated and unsaturated fatty acids, protein and fiber, and also for the majority of vitamins and calcium, as normalized by body weight. Interestingly, the elderly belonging to the G2 group showed a significantly higher carbohydrate intake (Kruskal–Wallis test,  $p$  value = 0.025; post-hoc Wilcoxon test,  $p$  value < 0.05 for G1 vs G2 and G2 vs G3) and a trend to higher levels of water (Kruskal–Wallis test,  $p$  value = 0.055), b-carotene ( $p$  value = 0.052) and

vitamin C ( $p$  value = 0.054). Moreover, by comparing the average daily intake (normalized to body weight) of different food groups among the three microbiome clusters, the elderly in the G2 group showed a significantly lower intake of potatoes than G1 (0.10 g/day vs 0.27 g/day for G1, post-hoc Wilcoxon test,  $p$  value < 0.05) and a trend to higher intake of fruit plus vegetables when compared with G3 (9.41 g/day vs 6.20 g/day for G3; Wilcoxon test,  $p$  value = 0.058) (Table S1). A superimposition analysis of the average daily intakes of food groups on the PCoA plot of Figure 1a confirmed an association between the microbiota profile of the G2 group and a lower consumption of potatoes along with cheese (permutational correlation test,  $p$  value  $\leq 0.025$ ) (Fig. S7).

Finally, serum metabolomics data were analyzed in order to find out metabolites that discriminated

**Table 2.** Average daily intake of energy and nutrients. All values were normalized to body weight (kg). Data are shown for the entire cohort as well as for the three microbiome groups (G1 to G3), as identified by PCoA of unweighted UniFrac distances (see Figure 1a). Values are expressed as mean (SD). *P* values were determined by Kruskal-Wallis test, followed by post-hoc Wilcoxon test. MUFA, monounsaturated fatty acids; PUFA, polyunsaturated fatty acids. ns, not significant.

	All (no. = 201)	G1 (no. = 147)	G2 (no. = 20)	G3 (no. = 34)	<i>p</i> value
Total energy (kcal)	24.44 (6.14)	24.25 (5.94)	27.41 (7.54)	23.52 (5.75)	ns
Total carbohydrates (g) <sup>#§</sup>	3.15 (0.95)	3.11 (0.87)	3.76 (1.23)	2.99 (0.95)	0.025
Total fats (g)	0.87 (0.24)	0.87 (0.24)	0.90 (0.26)	0.87 (0.25)	ns
Total saturated fatty acids (g)	0.27 (0.08)	0.27 (0.08)	0.28 (0.08)	0.27 (0.08)	ns
Total MUFA (g)	0.39 (0.12)	0.38 (0.12)	0.43 (0.15)	0.39 (0.10)	ns
Total PUFA (g)	0.12 (0.05)	0.12 (0.05)	0.12 (0.05)	0.12 (0.06)	ns
omega 3 PUFA (g)	0.01 (0.01)	0.01 (0.01)	0.01 (0.01)	0.01 (0.01)	ns
omega 6 PUFA (g)	0.07 (0.04)	0.07 (0.04)	0.08 (0.03)	0.08 (0.05)	ns
Total proteins (g)	0.95 (0.22)	0.95 (0.22)	1.00 (0.24)	0.90 (0.21)	ns
Animal proteins (g)	0.46 (0.14)	0.46 (0.15)	0.45 (0.13)	0.44 (0.13)	ns
Vegetal proteins (g)	0.35 (0.14)	0.35 (0.15)	0.39 (0.16)	0.32 (0.11)	ns
Total dietary fiber (g)	0.31 (0.15)	0.31 (0.15)	0.34 (0.16)	0.28 (0.14)	ns
Starch (g)	1.43 (0.55)	1.42 (0.56)	1.64 (0.61)	1.31 (0.45)	ns
Cholesterol (g)	2.89 (0.97)	2.91 (0.99)	2.96 (1.10)	2.77 (0.84)	ns
Water (g)	26.37 (9.41)	0.23 (0.99)	32.45 (12.19)	25.06 (7.93)	0.055
Biotin (mg)	0.25 (0.16)	0.26 (0.16)	0.23 (0.08)	0.24 (0.17)	ns
Folic acid (µg)	3.97 (1.76)	3.99 (1.68)	4.84 (2.53)	3.40 (1.36)	ns
b-carotene (µg)	25.10 (19.27)	24.72 (19.38)	34.41 (24.41)	21.26 (13.30)	0.052
Vitamin B1 (mg)	0.01 (0.01)	0.01 (0.01)	0.02 (0.01)	0.01 (0.01)	ns
Vitamin B2 (mg)	0.02 (0.01)	0.02 (0.01)	0.03 (0.01)	0.02 (0.01)	ns
Vitamin B3 (mg)	0.28 (0.15)	0.27 (0.14)	0.34 (0.23)	0.26 (0.14)	ns
Vitamin B5 (mg)	0.03 (0.01)	0.03 (0.01)	0.04 (0.02)	0.03 (0.01)	ns
Vitamin B6 (mg)	0.02 (0.01)	0.02 (0.01)	0.03 (0.01)	0.02 (0.01)	ns
Vitamin B12 (µg)	0.06 (0.06)	0.06 (0.06)	0.05 (0.06)	0.06 (0.08)	ns
Vitamin A (µg)	13.82 (10.23)	13.80 (10.19)	15.73 (10.61)	12.77 (10.32)	ns
Vitamin C (mg)	1.83 (1.16)	1.86 (1.10)	2.34 (1.82)	1.40 (0.76)	0.054
Vitamin D (µg)	0.03 (0.03)	0.03 (0.03)	0.04 (0.04)	0.03 (0.02)	ns
Vitamin E (mg)	0.13 (0.05)	0.13 (0.05)	0.15 (0.05)	0.13 (0.05)	ns
Calcium (mg)	10.44 (3.85)	10.34 (3.89)	11.45 (3.97)	10.26 (3.61)	ns

Post-hoc Wilcoxon test: <sup>#</sup>G1 vs G2, *p* value < 0.05; <sup>§</sup>G2 vs G3, *p* value < 0.05.

gut microbiome structures. The G2 group was characterized by significantly lower circulating levels of some serum metabolites, including mineral (sulfur), BCAAs (isoleucine, leucine and valine), fatty acids (myristic acid – C14:0) and methyl ester fatty acids (methyl-hexadecenoic acid, and tetramethyl-dihydroxy-octadecahexaenoic acid) (post-hoc Wilcoxon test for G2 vs G1 and/or G3, *p* value ≤ 0.05), and a tendency to lower levels of primary bile acid, chenodeoxycholic acid (*p* value > 0.05). On the other hand, methyl-heptadecadienoic acid was found to be significantly higher in G2 compared to G3, but also in G1 compared to G3 (*p* value ≤ 0.05) (Figure 3). Based on a sPLS regression analysis of relative abundances at the genus level and metabolites (Fig. S8), genera belonging to the families identified as signatures of the G2 group, *i.e.*, *Christensenellaceae* R7 group, *Alistipes* and *Parabacteroides*, inversely correlated with BCAAs, while some *Lachnospiraceae* and *Ruminococcaceae*

members, distinctive of the G1 and G3 profiles, showed opposite correlations. Similarly, for fatty acids, we observed negative correlations between *Christensenellaceae* R7 group or *Alistipes* and the majority of systemic fatty acids retained in the sPLS regression model. In contrast, mostly positive correlations were found with *Lachnospiraceae* taxa, along with *Bifidobacterium*, *Streptococcus*, *Ruminococcus 1* and *Erysipelotrichaceae* UCG 003.

## Discussion

In the present study, we identified three significantly different groups (G1 to G3) of elderly Italian individuals harboring distinct gut microbiome structures, which correlate with body composition and other health-related parameters. In particular, the G1 group was characterized by higher abundance of *Lachnospiraceae*, the G2 group was enriched in *Christensenellaceae*, *Porphyromonadaceae* and *Rikenellaceae*, and G3

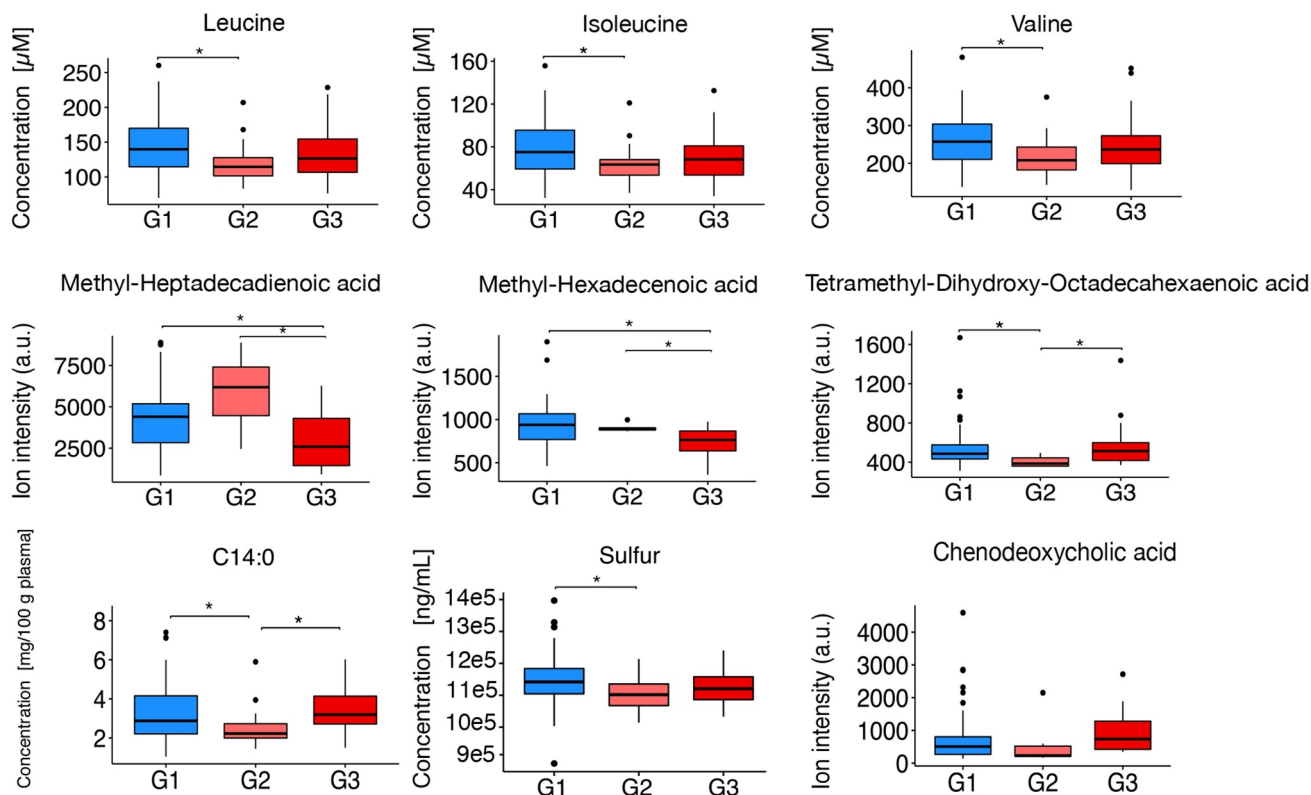


**Figure 3.** Serum metabolites discriminating for the elderly gut microbiome groups. Box-and-whisker plots showing the distribution of the circulating levels of branched-chain amino acids (*i.e.*, leucine, isoleucine and valine), fatty acids (methyl-heptadecadienoic acid, methyl-hexadecenoic acid and tetramethyl-dihydroxy-octadecahexaenoic acid), the saturated fatty acid, myristic acid (C14:0), mineral sulfur (S) and the primary bile acid, chenodeoxycholic acid. \*,  $p$  value  $\leq 0.05$ , Wilcoxon test.

in *Ruminococcaceae*. The three profiles were also characterized by different biodiversity, with G2 and G3 showing the highest level followed by G1. When we explored the connections between the gut microbiome and body composition, we found that the G2 microbiome cluster had the lowest median value of VAT, a specific measure of abdominal obesity.

Unlike a recent study in a Chinese adult population, which reported a sex-specific association between the gut microbiome layout and fat distribution, using DXA data for android and gynoid fat, the microbial communities defining the three elderly groups in our work are neither sex-related nor age-driven.<sup>28</sup> However, it should be noted that our dataset is constrained to old age and characterized by a lower range of android/gynoid to whole-fat mass ratio (the lowest and highest value in our cohort, 4.1 and 21.9, respectively; in the Chinese cohort, 6.6 and 26.6, respectively).

In line with the available literature, the microbial footprints of the G2 group (*i.e.*, the greater

proportion of *Christensenellaceae*, *Porphyromonadaceae* and *Rikenellaceae*) could contribute to a reduced amount of visceral fat mass.<sup>29,32,33</sup> Indeed, the family *Christensenellaceae* has been consistently reported as negatively related to visceral fat mass and indicated as a marker of lean phenotype,<sup>29,34,35</sup> as also shown by our sPLS regression. On the other hand, *Porphyromonadaceae* and *Rikenellaceae* members, both belonging to the Bacteroidetes phylum, could play a role as adiposity modulators through the production of the SCFAs acetate and propionate.<sup>36</sup> Specifically, it has been shown that acetate contributes to adiposity reduction in mice, by upregulating the genes involved in fatty acid oxidation in the liver.<sup>37</sup> Furthermore, the abundances of *Christensenellaceae* and *Rikenellaceae* have recently been found to be highly correlated with each other and significantly higher in lean than obese subjects.<sup>38</sup>

Conversely, the family *Lachnospiraceae*, found to be distinctive of the low-diverse,



higher VAT-related microbiome profile G1, has been connected to dietary lipid metabolism, and genera belonging to this family, e.g. *Blautia*, have been associated with higher amounts of VAT,<sup>29,39,40</sup> as in our correlation analysis. On the other hand, for members of *Ruminococcaceae* (marker of the high-diverse but VAT-related G3 group) we found conflicting trends of association with visceral fat, which are however generally consistent with what is available in the literature. For example, *Faecalibacterium*, which in our cohort positively correlated with VAT, has sometimes been found at increased levels in obese subjects, despite the known anti-inflammatory and immunomodulating properties, probably due to its ability to increase energy harvesting from otherwise unabsorbable carbohydrates.<sup>41,42</sup> In contrast, the genera *Ruminococcaceae* UCG 014 and *Ruminococcaceae* UCG 005 have both been negatively associated with adiposity,<sup>43,44</sup> in line with our sPLS regression. It is also worth noting that *Subdoligranulum*, which in our dataset showed positive associations with all DXA-related variables considered except SMI (a lean mass parameter), has recently been identified as one of the few key species associated with both fecal and blood metabolic profiles, therefore likely to play a major role in the gut-systemic metabolic interplay.<sup>45</sup>

Interestingly, while the entire cohort is composed of apparently healthy elderly subjects with almost all risk parameters in their normal range, the elderly in the G2 group, compared to G1 and G3, have a significantly lower level of several anthropometric, metabolic, cardiovascular and renal risk factors, such as BMI, waist and hip circumference and waist-to-hip ratio, diastolic pressure, creatinine and uric acid, and higher levels of adiponectin, an adipose-related cytokine with anti-inflammatory effects. These findings are of particular interest, also because *Christensenellaceae*, specifically enriched in G2 subjects, are considered an important component of the gut microbiome of centenarians and semi-supercentenarians, and of a healthier profile in general, thus potentially representing a marker of healthy aging and longevity since the early old age (60–70 years).<sup>11,46,47</sup>

Furthermore, compared to G1 and G3 groups, the elderly in G2 showed lower serum levels of BCAAs, which are known to be associated with insulin-deficient and – resistant disorders and have already been shown to correlate positively with VAT.<sup>48–50</sup> The G2 group was also characterized by lower circulating levels of methyl ester fatty acids and myristic acid, for which an inverse association with HDL cholesterol levels was demonstrated in an Italian population following a Mediterranean diet.<sup>51</sup> Although cholesterol levels are not discrete in the three groups, the mean values are lower for G2. As expected, both fatty acid and BCAA levels were found to inversely correlate with genera belonging to the families identified as signatures of the G2 group, *i.e.*, *Christensenellaceae* R7 group, *Alistipes* and *Parabacteroides*, while positively with some *Lachnospiraceae* and *Ruminococcaceae* members, distinctive of the G1 and G3 profiles. It is also worth noting that the elderly in the G2 group showed a tendency to lower levels of chenodeoxycholic acid, whose impact on cholesterol metabolism is not yet conclusive but could be unfavorable.<sup>52</sup> This could suggest a greater capacity of production of secondary bile acids by the G2-related gut microbiota. Although this ability must be verified by appropriate methods, including metagenomics, metatranscriptomics and, not least, stool metabolomics, previous reports have shown that G2 discriminating taxa, especially Bacteroidetes members, are capable of deconjugation and metabolism of primary bile acids into secondary ones.<sup>53–56</sup> Further strengthening this hypothesis, a strong positive correlation has recently been found between secondary bile acid metabolism and *Christensenellaceae*, another distinctive taxon of the G2 profile.<sup>57</sup> Based on a search in the PFAM and NCBI database, *Christensenellaceae* species actually exhibit both bile salt hydrolase (EC 3.5.1.24) and bile-acid 7- $\alpha$ -dehydratase (EC 4.2.1.106) activity, participating in the 7-dehydroxylation process associated with bile acid degradation.<sup>58,59</sup>

Consistent with the above assumptions of better metabolic health for the elderly in the G2 group, their dietary pattern was also healthier, with lower consumption of potatoes and a trend to higher average daily intake of fruit and vegetables than

the other groups. Interestingly, it has been demonstrated that increasing the consumption of fruit and vegetables and reducing the intake of potatoes can reduce the risk of ischemic stroke.<sup>60</sup> Furthermore, the G2-related microbiota profile was found to be associated with a lower intake of cheese, another well-known product to increase cardiovascular risk through adiposity and lipid pathways.<sup>61</sup>

In summary, here we advance the hypothesis that distinctive high-diverse structures of the gut microbiome of the elderly may contribute to a reduced amount of VAT. In particular, our results suggest the relevance of high amounts of *Christensenellaceae*, *Porphyromonadaceae* and *Rikenellaceae* as protective of cardiovascular and metabolic diseases related to visceral fat and, thus, potential markers of healthy aging and, possibly, longevity. This hypothesis is supported by a healthier dietary intake and metabolic profile, and overall better health for the elderly harboring this microbial layout. We can therefore argue that favorable compositions of the gut microbiota of older people could contribute to reduce metaflammation, a specific metabolism-induced inflammation, mostly overlapping with inflammaging, triggering obesity-induced insulin resistance and type 2 diabetes.<sup>62</sup>

Further studies in larger cohorts, possibly from different geographical locations, via shotgun metagenomics combined with metabolomics, will be needed to confirm our findings and provide insights on the mechanisms underlying the relationship between gut microbes and VAT, and their role in modulating adiposity and promoting a healthy life. Such mechanisms should possibly be validated in an animal model. Similarly, additional work, possibly also through culturomics approaches, is required to better understand the dynamics and ecological rules within the gut microbiota that lead to the establishment of different networks. It is reasonable to expect that in the near future the targeted manipulation of the elderly intestinal microbiota, the feasibility of which has been recently demonstrated in the context of NU-AGE,<sup>63</sup> will become an integral component of current strategies aimed at contrasting age-related deterioration in body composition and multiple bodily functions, thus supporting healthy aging.

## Materials and methods

### Study cohort

NU-AGE (<https://cordis.europa.eu/project/id/266486>) is a multicentre EU FP7 project, ended in 2016, which involved 30 partners from 16 European countries, working in the field of nutrition, gerontology, immunology and molecular biology. NU-AGE objective was to study the effects of a 12-month customized Mediterranean diet (registered with clinicaltrials.gov, NCT01754012) on the aging process, including cognitive decline, bone density, muscle mass, digestive health, immune and cardiovascular systems. Enrollment of participants has been described in detail previously.<sup>64,65</sup> Briefly, after screening for inclusion/exclusion criteria, 1,279 free-living healthy elderly aged 65 to 79 years were enrolled across five EU countries (Poland, Netherlands, UK, France, Italy) and thoroughly characterized for anthropometry, nutritional status, body composition, health and medical status, cognitive and physical functions, and a series of biochemical and inflammatory measures.<sup>66</sup> Participants were classified according to their frailty status based on the five criteria proposed by Fried and colleagues, including weight loss, weakness (*i.e.*, poor handgrip strength), self-reported exhaustion, slowness (*i.e.*, slow gait speed), and low physical activity. Only non-frail (absence of all the above 5 criteria) and pre-frail (presence of 1 or 2 of the criteria) subjects were included in the study.<sup>67</sup>

Written informed consent was collected from all participants prior to their inclusion in the study, in accordance with the Declaration of Helsinki. NU-AGE was approved by the ethics committee of the coordinator center – the Independent Ethics Committee of the S. Orsola-Malpighi Hospital Bologna (Italy) – and by the local/national ethics committees of all the other four recruiting centers.

As the analysis of VAT and SAT by DXA was only available for the Italian elderly, here we focused only on this cohort, of which we profiled the fecal microbiome by means of next-generation sequencing, and sought correlations with DXA variables, especially VAT and SAT, as well as with dietary habits and circulating metabolites (please see the paragraphs below). As for stool collection, each participant was asked to collect a fecal sample.

The samples were immediately stored at  $-20^{\circ}\text{C}$  and delivered to the Department of Experimental, Diagnostic and Specialty Medicine (University of Bologna, Bologna, Italy) where they were stored at  $-80^{\circ}\text{C}$  until processing.

### ***Anthropometric, physical, cardiovascular, clinical and cognitive function assessment***

Height was measured by a stadiometer to the nearest 0.1 cm. Weight was measured to the nearest 0.1 kg with a calibrated scale while wearing light clothes. Body Mass Index (BMI) was calculated as  $\text{weight}/\text{height}^2$  ( $\text{kg}/\text{m}^2$ ). Waist circumference was measured either at the narrowest circumference of the torso or at the midpoint between the lower ribs and the iliac crest. Hip circumference was measured horizontally at the level of the largest lateral extension of the hips or over the buttocks. Hand grip strength was measured three times in the dominant hand using the Scanditact Smedley's Hand Dynamometer® (Odder, Denmark) to the nearest 0.1 kg. Physical performance was evaluated by the sum score of 6-minute walking distance, Activities of Daily Living (ADL) scale, Instrumental Activities of Daily Living (IADL) scale and PASE questionnaire. Cognitive function was assessed by the administration of the Cambridge Mental Disorders of the Elderly Examination (CAMDEX) subjective memory score, the Geriatric Depression Scale (GDS) score and Mini Mental State Examination (MMSE) score as previously reported.<sup>68</sup> Blood pressure and heart rate were measured using the automated and calibrated electronic monitor Omron, M2 compact (Milan, Italy) as previously reported.<sup>69</sup> The use of prescribed medicines and supplements and the clinical history were collected by a questionnaire and verified by interviewers. All measures and questionnaires were taken by trained research assistants.

### ***Body composition assessment***

Direct measurements of total and regional body composition were obtained by performing whole body DXA scan (Lunar iDXA, GE Healthcare, Madison, WI – enCORE™ 2011 software version 13.6 and upgrade to estimate VAT and SAT). The scanners are compliant

with standard quality control procedures and were re-calibrated daily following the manufacturers' instructions. DXA scans were performed by trained personnel, removing all metal items prior to densitometry and placing the subjects in supine position with arms resting on the side of the participant's body, leaving some space with respect to the trunk and centered on the scanning field. DXA scanned the following regions: total body, trunk, upper limbs, lower limbs, android region (from the two superior iliac crests and extended cranially and covering 20% of the distance to the chin) and gynoid region (from the greater trochanter of the femur directed caudally and covering two times the distance in the android region). For each scanned region, the weight (in g) of the total mass, fat mass, non-bone lean mass and bone mineral content were obtained. Measurements of VAT and SAT were obtained at android level with CoreScan software.

This work includes variables related to total fat and lean mass distribution and bone mineral content, with a focus on fat measures of the abdominal area including subcutaneous and visceral adiposity: whole-body fat mass (FM, g), whole-body fat mass index (FMI,  $\text{g}/\text{m}^2$ ), whole-body fat mass to lean mass ratio (FM/LM), whole-body non-bone lean mass (LM, g), whole-body non-bone lean mass index (LMI,  $\text{g}/\text{m}^2$ ), skeletal mass index (SMI, *i.e.*, the appendicular lean mass to total body mass ratio), whole-body bone mineral content (BMC, g), whole-body bone mineral density (BMD,  $\text{g}/\text{cm}^2$ ), whole-body T-score (T-score), android fat mass to android lean mass ratio (AF/AL), android fat mass to gynoid fat mass ratio (AF/GF), VAT (g) and SAT (g) and their ratio.

### ***Blood sampling and biochemical parameters***

Blood samples were obtained after participants had fasted (at least 8 h) and had avoided heavy exercise and alcohol in the prior 24 h. Samples were centrifuged after sitting for 30 min at room temperature and separated into plasma and serum according to a standardized operating procedure, then aliquoted and stored at  $-80^{\circ}\text{C}$  until analysis.

Methods for inflammatory parameters assessment are reported in Santoro et al.<sup>69</sup> Briefly, C-reactive protein (CRP), leptin and adiponectin were measured by ProcartaPlex™ Immunoassay (Thermo Fisher Scientific, Waltham, MA, USA), performed using Luminex 200 instrumentation (Luminex Corporation, Austin, TX, USA), according to the manufacturer's instructions. Ghrelin and Pentraxin-3 were measured in multiplex with Bio-Plex Pro human diabetes and Pro human inflammation assay (Bio-Rad, Hercules, CA, USA), respectively. Plates were read and analyzed by Bio-Plex Manager Software (Bio-Rad). Plasma homocysteine was measured by an enzymatic assay using an Olympus AU400 clinical chemistry platform (Beckman Coulter, High Wycombe, UK). Serum glucose and serum insulin were determined by biochemical assay and chemiluminescent immunoassay, respectively. Insulin resistance status was calculated according to the homeostasis model assessment of insulin resistance (HOMA-IR) using the following formula:  $\text{insulin (mIU/mL)} \times \text{glucose (mmol/L)} / 22.5$ .<sup>70</sup> Plasma albumin was analyzed using the VITROS ALB slides (Ortho-Clinical Diagnostics, UK) on a VITROS 5.1/FS analyzer. Plasma total, High-Density Lipoprotein (HDL) and Low-Density Lipoprotein (LDL) cholesterol and triglycerides were measured on a Konelab system and reagents were from Thermo Scientific (Asnières sur Seine, France). All the other biochemical analyses, including creatinine, uric acid, alkaline phosphatase (ALP), gamma-glutamyl transpeptidase (GGT), aspartate aminotransferase (AST) and alanine transaminase (ALT) were measured on frozen blood and frozen urine (urea) in a centralized center with standard methodologies.

### **Dietary intake data**

Dietary intake was assessed by 7-day food records as reported elsewhere.<sup>71</sup> Briefly, participants were trained one to one by the interviewer receiving exhaustive instructions to correctly fill in the food diary. Food records were provided in a structured format, with tables for each day and eating occasion, time/hour, location, foods and drinks consumed, quantity and recipes in order to record all

details of the meals. Participants were recommended to record data at the time the foods were eaten/consumed and not to change eating habits during the week of registration. At the end of the recorded period, the 7-day food records were accurately checked to obtain more detailed information about types of foods, dressings, preparation methods and recipes, to estimate portion sizes by using real-life models and pictures and to probe the possible consumption of forgotten foods. Consumed foods were coded according to standardized procedures and translated into nutrients by the use of WinFood® software exploiting local food composition tables: INRAN (National Institute for Research on Food and Nutrition, Italy) and IEO (European Institute of Oncology, Italy). Energy (kcal), total carbohydrate (g), total protein (g), animal and plant protein (g), total, saturated and unsaturated fat (g), fiber (g) cholesterol (g), water (g), vitamin (mg: biotin, B1, B2, B3, B6, C, E; µg: folic acid, b-carotene, A, B12, D), and calcium (mg) intake normalized on body weight (g/kg BW), were used in the analysis together with the intake of food groups (white and whole grains, fruits and vegetables, legumes, dairy products, cheese, red and processed meat, white meat, nuts and seeds, potatoes, eggs and egg products, butter and animal fat, olive oil, other vegetable oils, sugar and sweetened beverages, sugar, honey and artificial sweeteners, sweet, chocolate and snacks) (g/day) normalized on body weight. The dietary intakes from the 7-day food records were added/summed to the intakes of related dietary supplements as assessed by a specific vitamin/mineral supplements questionnaire.

### **Serum metabolomics analysis**

Untargeted metabolomics was performed following the procedure described in Pujos-Guillot et al.<sup>72</sup> Briefly, serum samples (100 µL) were deproteinized using cold methanol. After evaporation under nitrogen, the dry residues were redissolved in 50/50 (v/v) acetonitrile/water containing 0.1% formic acid. Pooled quality-control samples were prepared by mixing 20 µL from each of the serum samples and prepared similarly. Metabolic profiles were then determined using an ultra-performance liquid chromatography coupled to quadrupole-time-of-



flight mass spectrometer (Bruker Impact HD2), equipped with an electrospray source. Separations were carried out using an Acquity HSS T3 column (Waters). Data were acquired in positive and negative ion modes with a scan range from 50 to 1,000 mass-to-charge ratio ( $m/z$ ). Data were processed under the Galaxy web-based platform Workflow4metabolomics using first XCMS, followed by quality checks and signal drift correction.<sup>73</sup> The remaining unknown compounds were identified on the basis of their exact masses which were compared to those registered in the Human Metabolome Database (HMDB) or in Kyoto Encyclopedia of Genes and Genomes (KEGG) database. Database results were confirmed using appropriate standards when available, isotopic patterns, and mass fragmentation analyses, performed on a Thermo Scientific LTQ Orbitrap Velos hybrid mass spectrometer (Thermo Fisher Scientific, San José, CA, USA) using high resolution, at 100,000 resolving power.

### **Microbial DNA extraction**

Microbial DNA was extracted from 250 mg of fecal material using the repeated bead-beating plus column method.<sup>74</sup> Briefly, samples were suspended in 1 mL of lysis buffer (500 mM NaCl, 50 mM Tris-HCl pH 8, 50 mM EDTA, and 4% SDS) and bead-beaten three times in the presence of four 3-mm glass beads and 0.5 g of 0.1-mm zirconia beads (BioSpec Products, Bartlesville, OK, USA), in a FastPrep instrument (MP Biomedicals, Irvine, CA, USA) at 5.5 movements/s for 1 min. Afterward, the samples were incubated at 95°C for 15 min and subsequently centrifuged for 5 min at 13,000 rpm. The supernatant was added with 260  $\mu$ L of 10 M ammonium acetate and incubated in ice for 5 min. After a further centrifugation step, one volume of isopropanol was added to the supernatant and incubated in ice for 30 min. Precipitated DNA was washed with 70% ethanol and resuspended in 100  $\mu$ L of TE buffer. The samples were depleted of RNA and proteins with 2  $\mu$ L of 10 mg/mL DNase-free RNase at 37°C for 15 min and 15  $\mu$ L of proteinase K (QIAGEN, Hilden, Germany) at 70°C for 10 min, respectively. Final DNA purification was performed using the QIAamp DNA Stool Mini Kit (QIAGEN). The purified nucleic acids

were quantified with the NanoDrop ND-1000 spectrophotometer (NanoDrop Technologies, Wilmington, DE, USA).

### **16S rRNA gene amplification and sequencing**

The V3–V4 hypervariable region of the 16S rRNA gene was PCR amplified with 341F and 805R primers with Illumina overhang adapter sequences as previously reported.<sup>75</sup> The PCR thermal cycle was as follows: denaturation at 95°C for 3 min, followed by 25 cycles of denaturation at 95°C for 30 s, annealing at 55°C for 30 s, then extension at 72°C for 30 s, and the last extension step at 72°C for 5 min. The Agencourt AMPure XP magnetic beads (Beckman Coulter, Brea, CA, USA) were used to clean PCR amplicons. Indexed libraries were obtained by limited-cycle PCR using Nextera technology. After a second clean-up as described above, libraries were pooled at equimolar concentration, denatured with 0.2 N NaOH and diluted to 6 pM. For sequencing, an Illumina MiSeq (Illumina, San Diego, CA, USA) platform was used with a 2  $\times$  250 bp paired-end protocol, following the manufacturer's instructions. Sequencing data are available at NCBI SRA under the BioProject ID: PRJNA661289.

### **Bioinformatics and biostatistics**

Sequencing read quality was assessed with Fastqc tool. High-quality read couples were joined together in a single read with PANDAsq tool and the resultant reads with length lower than 350 bp and greater than 500 bp were filtered out. Single-end reads were further pre-processed with DADA2, in order to reduce the noise of the dataset, eliminating chimera sequences and duplicates, and cluster them into amplicon sequence variants (ASVs).<sup>76,77</sup> The algorithm VSEARCH was applied to scan the representative feature sequences against the precomputed clusters from SILVA database (128 version) at 99% of sequence identity, and to assign the taxonomy with a confidence score > 0.5.<sup>78</sup> The ASVs table was normalized by the minimum number of feature sequences in a sample. Read pre-processing and taxonomic classification were performed in QIIME 2 (release 2018) framework.<sup>79</sup> The R packages Phyloseq and Vegan

were used for statistical analysis. Beta diversity was calculated with unweighted, weighted and generalized UniFrac metrics (GUniFrac package), and the function *adonis* was used to test the significance of beta diversity-based sample separation in Principal Coordinates Analysis (PCoA).<sup>80,81</sup> The separation of the three microbiome groups (G1 to G3) as found in the unweighted UniFrac-based PCoA was verified by means of hierarchical clustering with Ward as the linkage method. The congruence between PCoA groups and the hierarchical clustering separation was verified by Fisher's exact test. The stability of the clusters was assessed by using average Jaccard similarities from the *clusterboot* function in the R package *fpc*. Alpha diversity was estimated using the number of observed ASVs and Chao1 index. Power calculation was computed with *micropower* R package;<sup>82</sup> we found that the size of G1 to G3 microbiome groups allowed 90% power to detect an  $\omega^2$  of 0.014.

To find associations between the gut microbiota profiles and host characteristics, we adopted the sparse partial least square (sPLS) regression analysis as implemented in the *mixOmics* package in R, modeling the genus-level relative abundances to the DXA measures or metabolite classes via multiple regressions.<sup>83</sup> The number of components was tuned to 2, with *perf* function, retaining all DXA/metabolomic variables and all taxa in the model. Bacterial abundances were transformed as Centered Log Ratio (CLR). The associations between genera and DXA/metabolomic matrices were visualized projecting the variables inside a correlation circle plot (*plotVar*), with associated variables projected in the same direction.<sup>84</sup> Hierarchical clustering (*cim*) on the sPLS regression model was plotted with Pearson correlation as distance and complete linkage method. As for diet, the food groups most contributing to the PCoA ordination space were identified using the function "envfit" of *vegan*. Significant differences among the microbiota groups identified by PCoA in taxon relative abundance as well as in measures of DXA-related variables, dietary and metabolomics data and other health-related parameters, were assessed using the Kruskal-

Wallis test. Wilcoxon test was adopted as a post-hoc test to check for differences between each pair of groups, adjusting *p* values for multiple testing via Benjamini–Hochberg method. A *p* value  $\leq 0.05$  was considered statistically significant.

## Acknowledgments

The NU-AGE project was supported by the European Union's Seventh Framework Programme under grant agreement no. 266486 ('NU-AGE: New dietary strategies addressing the specific needs of the elderly population for healthy ageing in Europe'). This work was partially supported by Russian Ministry of Science and Education Agreement No. 13.1902.21.0026 to C.F. We thank Dr. Daniele Mercatelli from the diagnostic and interventional Radiology of the IRCCS Istituto Ortopedico Rizzoli in Bologna for his valuable support in the DXA data organization.

## Author contributions

A.S. and S.R., conceptualization; A.S., S.R. and S.T., project administration; P.B. and C.F., resources; M.B. and S.T., library preparation and sequencing; T.T. and S.R., bioinformatic and biostatistic analysis; A.B. G.B. and C.G., DXA analysis; C.N., F. K. and P.O.T. collected and contributed to data; A.S. S.S. and G.G., analysis of demographic, biochemical, nutritional and other health-related data; E.P.-G. and B.C., serum metabolomics; T.T., S.R., S.T. and A.S., writing - original draft; E. P.-G. and B.C., writing - review & editing. All authors discussed the results and commented on the manuscript.

## Disclosure of potential of interest

The authors declare no competing interests.

## Funding

This work was supported by the Seventh Framework Programme [266486] and by the JPI-HDHL INTIMIC METADIS [1164]

## ORCID

Estelle Pujos-Guillot  <http://orcid.org/0000-0002-4693-5712>

Paul W. O'Toole  <http://orcid.org/0000-0001-5377-0824>

Silvia Turrone  <http://orcid.org/0000-0003-2345-9482>

Aurelia Santoro  <http://orcid.org/0000-0002-7187-1116>

## References

1. Cani PD, Van Hul M, Lefort C, Depommier C, Rastelli M, Everard A. Microbial regulation of organismal energy homeostasis. *Nat Metab.* 2019;1(1):34–46. doi:10.1038/s42255-018-0017-4.
2. Spanogiannopoulos P, Bess EN, Carmody RN, Turnbaugh PJ. The microbial pharmacists within us: a metagenomic view of xenobiotic metabolism. *Nat Rev Microbiol.* 2016;14(5):273. doi:10.1038/nrmicro.2016.17.
3. Kim D, Zeng MY, Núñez G. The interplay between host immune cells and gut microbiota in chronic inflammatory diseases. *Exp & Molecular Medicine.* 2017;49(5):e339–e339. doi:10.1038/emm.2017.24.
4. Claesson MJ, Jeffery IB, Conde S, Power SE, O’connor EM, Cusack S, Harris HMB, Coakley M, Lakshminarayanan B, O’sullivan O, et al. Gut microbiota composition correlates with diet and health in the elderly. *Nature.* 2012;488(7410):178–184. doi:10.1038/nature11319.
5. Biagi E, Nylund L, Candela M, Ostan R, Bucci L, Pini E, Nikkila J, Monti D, Satokari R, Franceschi C, et al. Through ageing, and beyond: gut microbiota and inflammatory status in seniors and centenarians. *PLoS One.* 2010;5(6):5. doi:10.1371/journal.pone.0010667.
6. Ventura MT, Casciaro M, Gangemi S, Buquicchio R. Immunosenescence in aging: between immune cells depletion and cytokines up-regulation. *Clin Mol Allergy.* 2017;15(1):21. doi:10.1186/s12948-017-0077-0.
7. Nicoletti C. Age-associated changes of the intestinal epithelial barrier: local and systemic implications. *Expert Rev Gastroenterol Hepatol.* 2015;9(12):1467–1469. doi:10.1586/17474124.2015.1092872.
8. Villa CR, Ward WE, Comelli EM. Gut microbiota-bone axis. *Crit Reviews Food Science Nutrition.* 2017;57(8):1664–1672. doi:10.1080/10408398.2015.1010034.
9. Leung K, Thuret S. Gut microbiota: a modulator of brain plasticity and cognitive function in ageing. *Healthcare.* 2015;3(4):898–916. doi:10.3390/healthcare3040898.
10. Rampelli S, Candela M, Turrioni S, Biagi E, Collino S, Franceschi C, O’Toole PW, Brigidi P. Functional metagenomic profiling of intestinal microbiome in extreme ageing. *Aging.* 2013;5(12):902–912. doi:10.18632/aging.100623.
11. Biagi E, Franceschi C, Rampelli S, Severgnini M, Ostan R, Turrioni S, Consolandi C, Quercia S, Scurti M, Daniela MCM, et al. Gut microbiota and extreme longevity. *Curr Biol.* 2016;26(11):1480–1485. doi:10.1016/j.cub.2016.04.016.
12. Santoro A, Ostan R, Candela M, Biagi E, Brigidi P, Capri M, Franceschi C. Gut microbiota changes in the extreme decades of human life: a focus on centenarians. *Cell Molecular Life Sciences.* 2018;75(1):129–148. doi:10.1007/s00018-017-2674-y.
13. Santoro A, Bazzocchi A, Guidarelli G, Ostan R, Giampieri E, Mercatelli D, Scurti M, Berendsen A, Surala O, Jennings A, et al. A cross-sectional analysis of body composition among healthy elderly from the european NU-AGE study: sex and country specific features. *Front Physiol.* 2018;9:1693. doi:10.3389/fphys.2018.01693.
14. St-Onge MP, Gallagher D. Body composition changes with aging: the cause or the result of alterations in metabolic rate and macronutrient oxidation? *Nutrition.* 2010;26(2):152–155. doi:10.1016/j.nut.2009.07.004.
15. Reinders I, Visser M, Schaap L. Body weight and body composition in old age and their relationship with frailty. *Curr Opin Clin Nutr Metab Care.* 2017;20(1):11–15. doi:10.1097/MCO.0000000000000332.
16. Bazzocchi A, Diano D, Ponti F, Andreone A, Sassi C, Albisinni U, Marchesini G, Battista G. Health and ageing: A cross-sectional study of body composition. *Clin Nutr.* 2013;32(4):569–578. doi:10.1016/j.clnu.2012.10.004.
17. Ponti F, Santoro A, Mercatelli D, Gasperini C, Conte M, Martucci M, Sangiorgi L, Franceschi C, Aging BA. Imaging assessment of body composition: from fat to facts. *Front Endocrinol.* 2020;10:861. doi:10.3389/fendo.2019.00861.
18. Conte M, Martucci M, Sandri M, Franceschi C, Salvioli S. The dual role of the pervasive “fattish” tissue remodeling with age. *Front Endocrinol.* 2019;10:114. doi:10.3389/fendo.2019.00114.
19. Bunkin DAGAFS. Omental and subcutaneous adipose tissues of obese subjects release interleukin-6: depot difference and regulation by glucocorticoid. *J Clin Endocrinol Metab.* 1998;83(3):847–850. doi:10.1210/jcem.83.3.4660.
20. Kanda H, Tateya S, Tamori Y, Kotani K, Hiasa KI, Kitazawa R, Kitazawa S, Miyachi H, Maeda S, Egashira K, et al. MCP-1 contributes to macrophage infiltration into adipose tissue, insulin resistance, and hepatic steatosis in obesity. *J Clin Investig.* 2006;116(6):1494–1505. doi:10.1172/JCI26498.
21. Sato F, Maeda N, Yamada T, Namazui H, Fukuda S, Natsukawa T, Nagao H, Murai J, Masuda S, Tanaka Y, et al. *Circ J.* 2018;82(2):502–508. doi:10.1253/circj.CJ-17-0820.
22. Aparisi Gómez MP, Ponti F, Mercatelli D, Gasperini C, Napoli A, Battista G, Cariani S, Marchesini G, Bazzocchi A. Correlation between DXA and laboratory parameters in normal weight, overweight, and obese patients. *Nutrition.* 2019;61:143–150. doi:10.1016/j.nut.2018.10.023.
23. Turnbaugh PJ, Ley RE, Mahowald MA, Magrini V, Mardis ER, Gordon JI. An obesity-associated gut microbiome with increased capacity for energy harvest.

- Nature. 2006;444(7122):1027–1031. doi:10.1038/nature05414.
24. Turnbaugh PJ, Bäckhed F, Fulton L, Gordon JL. Diet-induced obesity is linked to marked but reversible alterations in the mouse distal gut microbiome. *Cell Host Microbe*. 2008;3(4):213–223. doi:10.1016/j.chom.2008.02.015.
  25. Ridaura VK, Faith JJ, Rey FE, Cheng J, Duncan AE, Kau AL, Grif- Fin NW, Lombard V, Henrissat B, Bain JR, et al. Gut microbiota from twins discordant for obesity modulate metabolism in mice. *Science*. 2013;341(6150):1241214. doi:10.1126/science.1241214.
  26. Rampelli S, Guenther K, Turroni S, Wolters M, Veidebaum T, Kourides Y, Molnár D, Ler L, Benitez-Paez A, Sanz Y, et al. Pre- obese children’s dysbiotic gut microbiome and unhealthy diets may predict the development of obesity. *Commun Biol*. 2018;1(1):222. doi:10.1038/s42003-018-0221-5.
  27. Canello R, Turroni S, Rampelli S, Cattaldo S, Candela M, Cattani L, Mai S, Vietti R, Scacchi M, Brigidi P, et al. Effect of short- term dietary intervention and probiotic mix supplementation on the gut microbiota of elderly obese women. *Nutrients*. 2019;11(12):3011. doi:10.3390/nu11123011.
  28. Min Y, Ma X, Sankaran K, Ru Y, Chen L, Baiocchi M, Zhu S. Sex-specific association between gut microbiome and fat distribution. *Nat Commun*. 2019;10(1):2408. doi:10.1038/s41467-019-10440-5.
  29. Beaumont M, Goodrich JK, Jackson MA, Yet I, Davenport ER, Vieira-Silva S, Debelius J, Pallister T, Mangino M, Raes J, et al. Heritable components of the human fecal microbiome are associated with visceral fat. *Genome Biol*. 2016;17(1):189. doi:10.1186/s13059-016-1052-7.
  30. Guglielmi G, Bazzocchi A. Body composition imaging. *Quant Imaging Med Surg*. 2020;10(8):1576–1579. doi:10.21037/qims-2019-bc-13.
  31. Messina C, Albano D, Gitto S, Tofanelli L, Bazzocchi A, Ulivieri FM, Guglielmi G, Sconfienza LM. Body composition with dual energy X-ray absorptiometry: from basics to new tools. *Quant Imaging Med Surg*. 2020;10(8):1687–1698. doi:10.21037/qims.2020.03.02.
  32. Bilsborough JC, Greenway K, Opar D, Livingstone S, Cordy J, Coutts AJ. The accuracy and precision of DXA for assessing body composition in team sport athletes. *J Sports Sci*. 2014;32(19):1821–1828. doi:10.1080/02640414.2014.926380.
  33. Tamura M, Hoshi C, Kobori M, Takahashi S, Tomita J, Nishimura M, Nishihira J. Quercetin metabolism by fecal microbiota from healthy elderly human subjects. *PLoS One*. 2017;12(11):e0188271. doi:10.1371/journal.pone.0188271.
  34. Menni C, Jackson MA, Pallister T, Steves CJ, Spector TD, Valdes AM. Gut microbiome diversity and high-fibre intake are related to lower long-term weight gain. *Int J Obes*. 2017;41(7):1099–1105. doi:10.1038/ijo.2017.66.
  35. Goodrich JK, Waters JL, Poole AC, Sutter JL, Koren O, Blekhman R, Beaumont M, Van Treuren W, Knight R, Bell JT, et al. Human genetics shape the gut microbiome. *Cell*. 2014;159(4):789–799. doi:10.1016/j.cell.2014.09.053.
  36. Lu Y, Fan C, Li P, Lu Y, Chang X, Qi K. Short chain fatty acids prevent high-fat-diet-induced obesity in mice by regulating g protein- coupled receptors and gut microbiota. *Sci Reports*. 2016;6(1):37589. doi:10.1038/srep37589.
  37. Kondo T, Kishi M, Fushimi T, Kaga T. Acetic acid upregulates the expression of genes for fatty acid oxidation enzymes in liver to suppress body fat accumulation. *J Agric Food Chem*. 2009;57(13):5982–5986. doi:10.1021/jf900470c.
  38. Oki K, Toyama M, Banno T, Chonan O, Benno Y, Watanabe K. Comprehensive analysis of the fecal microbiota of healthy Japanese adults reveals a new bacterial lineage associated with a phenotype characterized by a high frequency of bowel movements and a lean body type. *BMC Microbiol*. 2016;16(1):1–13. doi:10.1186/s12866-016-0898-x.
  39. Just S, Mondot S, Ecker J, Wegner K, Rath E, Gau L, Streidl T, Hery- Arnaud G, Schmidt S, Lesker TR, et al. The gut microbiota drives the impact of bile acids and fat source in diet on mouse metabolism. *Microbiome*. 2018;6(1):134. doi:10.1186/s40168-018-0510-8.
  40. Ozato N, Saito S, Yamaguchi T, Katashima M, Tokuda I, Sawada K, Katsuragi Y, Kakuta M, Imoto S, Ihara K, et al. Blautia genus associated with visceral fat accumulation in adults 20–76 years of age. *Npj Biofilms Microbiomes*. 2019;5(1):1. doi:10.1038/s41522-019-0101-x.
  41. Balamurugan R, George G, Kabeerdoss J, Hepsiba J, Chandragunasekaran A, Ramakrishna B. Quantitative differences in intestinal faecalibacterium prausnitzii in obese Indian children. *British Journal of Nutrition*. 2010;103(3):335–338. doi:10.1017/S0007114509992182.
  42. Del Chierico F, Abbatini F, Russo A, Quagliariello A, Reddel S, Capoccia D, Caccamo R, Ginanni Corradini S, Nobili V, De Peppo F, et al. Gut microbiota markers in obese adolescent and adult patients: age-dependent differential patterns. *Front Microbiol*. 2018;9:1210. doi:10.3389/fmicb.2018.01210.
  43. Wutthi-in M, Cheevadhanarak S, Yasom S, Kerdphoo S, Thiennimitr P, Phrommintikul A, Chattapakorn N, Kittichotirat W, Chattapakorn S. Gut microbiota profiles of treated metabolic syndrome patients and their relationship with metabolic health. *Sci Rep*. 2020;10(1):10085. doi:10.1038/s41598-020-67078-3.
  44. Zhao L, Zhang Q, Ma W, Tian F, Shen H, Zhou M. A combination of quercetin and resveratrol reduces obesity in high-fat diet-fed rats by modulation of gut microbiota. *Food Funct*. 2017;8(12):4644–4656. doi:10.1039/c7fo01383c.



45. Visconti A, Le Roy CI, Rosa F, Rossi N, Martin TC, Mohney RP, Li W, de Rinaldis E, Bell JT, Venter JC, et al. Interplay between the human gut microbiome and host metabolism. *Nat Commun.* 2019;10(1):4505. doi:10.1038/s41467-019-12476-z.
46. Waters JL, Ley RE. The human gut bacteria christensenellaceae are widespread, heritable, and associated with health. *BMC Biology.* 2019;17(1):1. doi:10.1186/s12915-019-0699-4.
47. Le Roy CI, Bowyer RCE, Castillo-Fernandez JE, Pallister T, Menni C, Steves CJ, Berry SE, Spector TD, Bell JT. Dissecting the role of the gut microbiota and diet on visceral fat mass accumulation. *Sci Reports.* 2019;9(1):9758. doi:10.1038/s41598-019-46193-w.
48. Holeček M. Branched-chain amino acids in health and disease: metabolism, alterations in blood plasma, and as supplements. *Nutrition & Metabolism.* 2018;15(1):1. doi:10.1186/s12986-018-0271-1.
49. Rietman A, Stanley TL, Clish C, Mootha V, Mensink M, Grinspoon SK, Makimura H. Associations between plasma branched-chain amino acids,  $\beta$ -aminoisobutyric acid and body composition. *Journal of Nutritional Science.* 2016;5:5. doi:10.1017/jns.2015.37.
50. Lackey DE, Lynch CJ, Olson KC, Mostaedi R, Ali M, Smith WH, Karpe F, Humphreys S, Bedinger DH, Dunn TN, et al. Regulation of adipose branched-chain amino acid catabolism enzyme expression and cross-adipose amino acid flux in human obesity. *Am J Physiol - Endocrinol Metab.* 2013;304(11):11. doi:10.1152/ajpendo.00630.2012.
51. Noto D, Fayer F, Cefalù AB, Altieri I, Palesano O, Spina R, Valenti V, Pitrone M, Pizzolanti G, Barbagallo CM, et al. Myristic acid is associated to low plasma HDL cholesterol levels in a mediterranean population and increases HDL catabolism by enhancing HDL particles trapping to cell surface proteoglycans in a liver hepatoma cell model. *Atherosclerosis.* 2016;246:50–56. doi:10.1016/j.atherosclerosis.2015.12.036.
52. Porez G, Prawitt J, Gross B, Staels B. Bile acid receptors as targets for the treatment of dyslipidemia and cardiovascular disease. *J Lipid Res.* 2012;53(9):1723–1737. doi:10.1194/jlr.R024794.
53. Hirano S, Masuda N. Enhancement of the 7 alpha-dehydroxylase activity of a gram-positive intestinal anaerobe by bacteroides and its significance in the 7-dehydroxylation of ursodeoxycholic acid. *J Lipid Res.* 1982;23(8):1152–1158. doi:10.1016/S0022-2275(20)38052-4.
54. Ishii M, Toda T, Ikarashi N, Kusunoki Y, Kon R, Ochiai W, Machida Y, Sugiyama K. Gastrectomy increases the expression of hepatic cytochrome P450 3A by increasing lithocholic acid-producing enteric bacteria in mice. *Biol Pharm Bull.* 2014;37(2):298–305. doi:10.1248/bpb.b13-00824.
55. Gu Y, Wang X, Li J, Zhang Y, Zhong H, Liu R, Zhang D, Feng Q, Xie X, Hong J, et al. Analyses of gut microbiota and plasma bile acids enable stratification of patients for antidiabetic treatment. *Nat Commun.* 2017;8(1):1785. doi:10.1038/s41467-017-01682-2.
56. Yao L, Seaton SC, Ndousse-Fetter S, Adhikari AA, DiBenedetto N, Mina AI, Banks AS, Bry L, Devlin AS. A selective gut bacterial bile salt hydrolase alters host metabolism. *Elife.* 2018;7:e37182. doi:10.7554/eLife.37182.
57. Alemán JO, Bokulich NA, Swann JR, Walker JM, De Rosa JC, Battaglia T, Costabile A, Pechlivanis A, Liang Y, Breslow JL, et al. Fecal microbiota and bile acid interactions with systemic and adipose tissue metabolism in diet-induced weight loss of obese postmenopausal women. *J Transl Med.* 2018;16(1):244. doi:10.1186/s12967-018-1619-z.
58. El-Gebali S, Mistry J, Bateman A, Eddy SR, Luciani A, Potter SC, Qureshi M, Richardson LJ, Salazar GA, Smart A, et al. The Pfam protein families database in 2019. *Nucleic Acids Res.* 2019;47(D1):D427–D432. doi:10.1093/nar/gky995.
59. NCBI Resource Coordinators. Database resources of the national center for biotechnology information. *Nucleic Acids Res.* 2018;46(D1):D8–D13. doi:10.1093/nar/gkx1095.
60. Hansen M, Würtz A, Hansen C, Tjønneland A, Rimm E, Johnsen S, Schmidt E, Overvad K, Jakobsen M. Substitutions between potatoes and other vegetables and risk of ischemic stroke. 2020. *Eur J Nutr.* Apr 9. published online ahead of print 10.1007/s00394-020-02237-w.
61. Trichia E, Luben R, Khaw KT, Wareham NJ, Imamura F, Forouhi NG. The associations of longitudinal changes in consumption of total and types of dairy products and markers of metabolic risk and adiposity: findings from the european investigation into cancer and nutrition (epic)-norfolk study, united kingdom. *Am J Clin Nutr.* 2020;111(5):1018–1026. doi:10.1093/ajcn/nqz335.
62. Franceschi C, Garagnani P, Parini P, Giuliani C, Santoro A. Inflammaging: a new immune-metabolic viewpoint for age-related diseases. *Nat Rev Endocrinol.* 2018;14(10):576–590. doi:10.1038/s41574-018-0059-4.
63. Ghosh TS, Rampelli S, Jeffery IB, Santoro A, Neto M, Capri M, Giampieri E, Jennings A, Candela M, Turroni S, et al. Mediterranean diet intervention alters the gut microbiome in older people reducing frailty and improving health status: the NU-AGE 1-year dietary intervention across five european countries. *Gut.* 2020;69(7):1218–1228. doi:10.1136/gutjnl-2019-319654.
64. Santoro A, Pini E, Scurti M, Palmas G, Berendsen A, Brzozowska A, Pietruszka B, Szczecinska A, Cano N, Meunier N, et al. Combating inflammaging through a mediterranean whole diet approach: the NU-AGE project's conceptual framework and design. *Mech*

- Ageing Dev. 2014;136-137:3–13. doi:10.1016/j.mad.2013.12.001.
65. Marseglia A, Wang HX, Rizzuto D, Fratiglioni L, Xu W. Participating in mental, social, and physical leisure activities and having a rich social network reduce the incidence of diabetes-related dementia in a cohort of Swedish older adults. *Diabetes Care*. 2019;42(2):232–239. doi:10.2337/dc18-1428.
66. Fried LP, Tangen CM, Walston J, Newman AB, Hirsch C, Gottdiener J, Seeman T, Tracy R, Kop WJ, Burke G, et al. Frailty in older adults: evidence for a phenotype. *The Journals Gerontol Ser A: Biol Sci Med Sci*. 2001;56(3):M146–M157. doi:10.1093/gerona/56.3.m146.
67. Marseglia A, Xu W, Fratiglioni L, Fabbri C, Berendsen AAM, Bialecka-Debek A, Jennings A, Gillings R, Meunier N, Caumon E, et al. Effect of the NU-AGE diet on cognitive functioning in older adults: A randomized controlled trial. *Front Physiol*. 2018;9:349. doi:10.3389/fphys.2018.00349.
68. Jennings A, Berendsen AM, LCPGM DG, Feskens EJM, Brzozowska A, Sicinska E, Pietruszka B, Meunier N, Caumon E, Malpuech-Brugère C, et al. Mediterranean-style diet improves systolic blood pressure and arterial stiffness in older adults: results of a 1-year european multi-center trial. *Hypertension*. 2019;73(3):578–586. doi:10.1161/HYPERTENSIONAHA.118.12259.
69. Santoro A, Guidarelli G, Ostan R, Giampieri E, Fabbri C, Bertarelli C, Nicoletti C, Kadi F, LCPGM DG, Feskens E, et al. Gender-specific association of body composition with inflammatory and adipose-related markers in healthy elderly europeans from the NU-AGE study. *Eur Radiol*. 2019;29(9):4968–4979. doi:10.1007/s00330-018-5973-2.
70. Matthews DR, Hosker JP, Rudenski AS, Naylor BA, Treacher DF, Turner RC. Homeostasis model assessment: insulin resistance and beta-cell function from fasting plasma glucose and insulin concentrations in man. *Diabetologia*. 1985;28(7):412–419. doi:10.1007/BF00280883.
71. Ostan R, Guidarelli G, Giampieri E, Lanzarini C, Berendsen AAM, Januszko O, Jennings A, Lyon N, Caumon E, Gillings R, et al. Cross-sectional analysis of the correlation between daily nutrient intake assessed by 7-day food records and biomarkers of dietary intake among participants of the NU-AGE study. *Front Physiol*. 2018;9:1359. doi:10.3389/fphys.2018.01359.
72. Pujos-Guillot E, Pétéra M, Jacquemin J, Centeno D, Lyan B, Montoliu I, Madej D, Pietruszka B, Fabbri C, Santoro A, et al. Identification of pre-frailty sub-phenotypes in elderly using metabolomics. *Front Physiol*. 2019;9:1903. doi:10.3389/fphys.2018.01903.
73. Giacomoni F, Le Corguillé G, Monsoor M, Landi M, Pericard P, Pétéra M, Duperier C, Tremblay-Franco M, Martin JF, Jacob D, et al. Workflow4Metabolomics: A collaborative research infrastructure for computational metabolomics. *Bioinformatics*. 2015;31(9):1493–1495. doi:10.1093/bioinformatics/btu813.
74. Yu Z, Morrison M. Improved extraction of PCR-quality community DNA from digesta and fecal samples. *BioTechniques*. 2004;36(5):808–812. doi:10.2144/04365ST04.
75. Barone M, Turrioni S, Rampelli S, Soverini M, D’Amico F, Biagi E, Brigidi P, Troiani E, Candela M. Gut microbiome response to a modern paleolithic diet in a western lifestyle context. *PLoS One*. 2019;14(8):e0220619. doi:10.1371/journal.pone.0220619.
76. Masella AP, Bartram AK, Truszkowski JM, Brown DG, Neufeld JD. PANDAseq: paired-end assembler for illumina sequences. *BMC Bioinform*. 2012;13(1):31. doi:10.1186/1471-2105-13-31.
77. Callahan BJ, McMurdie PJ, Rosen MJ, Han AW, Johnson AJA, Holmes SP. DADA2: high-resolution sample inference from Illumina amplicon data. *Nat Methods*. 2016;13(7):581–583. doi:10.1038/nmeth.3869.
78. Quast C, Pruesse E, Yilmaz P, Gerken J, Schweer T, Yarza P, Peplies J, Glöckner FO. The SILVA ribosomal RNA gene database project: improved data processing and web-based tools. *Nucleic Acids Res*. 2013;41(Database issue):D590–D596. doi:10.1093/nar/gks1219.
79. Bolyen E, Rideout JR, Dillon MR, Bokulich NA, Abnet CC, Al-Ghalith GA, Alexander H, Alm EJ, Arumugam M, Asnicar F, et al. Reproducible, interactive, scalable and extensible microbiome data science using QIIME 2. *Nat Biotechnol*. 2019;37(8):852–857. doi:10.1038/s41587-019-0209-9.
80. McMurdie PJ, Holmes S. phyloseq: an R package for reproducible interactive analysis and graphics of microbiome census data. *PLoS One*. 2013;8(4):e61217. doi:10.1371/journal.pone.0061217.
81. Dixon P. VEGAN, a package of R functions for community ecology. *J Veg Sci*. 2003;14(6):927–930. doi:10.1111/j.1654-1103.2003.tb02228.x.
82. Kelly BJ, Gross R, Bittinger K, Sherrill-Mix S, Lewis JD, Collman RG, Bushman FD, Li H. Power and sample-size estimation for microbiome studies using pairwise distances and PERMANOVA. *Bioinformatics*. 2015;31(15):2461–2468. doi:10.1093/bioinformatics/btv183.
83. Lê Cao K, Martin PG, Robert-Granié C, Besse P. Sparse canonical methods for biological data integration: application to a cross-platform study. *BMC Bioinform*. 2009;34:10. doi:10.1186/1471-2105-10-34.
84. González I, Cao KA, Davis MJ, Déjean S. Visualising associations between paired ‘omics’ data sets. *BioData Min*. 2012 Nov 13;5(1):19. doi:10.1186/1756-0381-5-19.